



Submitted: 18.10.2022
Accepted: 06.12.2022
Early publication date: 08.05.2023

Endokrynologia Polska
DOI: 10.5603/EPa2023.0020
ISSN 0423-104X, e-ISSN 2299-8306

MicroRNA-646 inhibits the proliferation of ovarian granulosa cells via insulin-like growth factor 1 (IGF-1) in polycystic ovarian syndrome (PCOS)

Jiali Lu¹, Feilan Xuan², Aixue Chen³, Ruiying Jin⁴, Weimei Zhou⁵, Yongju Ye⁶, Yuefang Ren¹

¹Department of Gynaecology, Huzhou Maternity and Child Health Care Hospital, Huzhou, China

²Department of Obstetrics and Gynaecology, Hangzhou Traditional Chinese Medical Hospital Affiliated to Zhejiang Chinese Medical University, Hangzhou, China

³Department of Gynaecology, Changxing People's Hospital of Chongming District, Shanghai, China

⁴Department of Gynaecology, Jiaojiang maternal and Child Health Hospital, Taizhou, China

⁵Department of Ultrasound, Jiaojiang Maternal and Child Health Hospital, Taizhou, China

⁶Department of Gynaecology, Lishui Hospital of Traditional Chinese Medicine, Lishui, China

Abstract

Introduction: Polycystic ovarian syndrome (PCOS) is a common endocrinopathy in women. MicroRNAs (miRNAs) have been proven to play a crucial role in balancing the proliferation and apoptosis of granulosa cells (GCs) in PCOS.

Material and methods: The miRNA of PCOS was screened by bioinformatics analysis, and microRNA 646 (miR-646) was found to be involved in insulin-related pathways by enrichment analysis. The cell counting kit-8 (CCK-8), cell colony formation, and the 5-ethynyl-2'-deoxyuridine (EdU) assays were used to explore the effect of miR-646 on proliferation of GCs, flow cytometry was used to measure the cell cycle and apoptosis, and Western blot and quantitative real-time polymerase chain reaction (qRT-PCR) were used to explore the biological mechanism of miR-646. The human ovarian granulosa cells KGN were selected by measuring the miR-646 and via insulin-like growth factor 1 (IGF-1) levels and used for cell transfection.

Results: Overexpressed miR-646 inhibited KGN cell proliferation, and silenced miR-646 advanced it. Most cells were arrested in the S phase of cell cycle with overexpressed-miR-646, while after silencing miR-646, cells were arrested in the G2/M phase. And the miR-646 mimic raised apoptosis in KGN cells. Also, a dual-luciferase reporter proved the regulation effect of miR-646 on IGF-1, miR-646 mimic inhibited IGF-1, and miR-646 inhibitor advanced IGF-1. The cyclin D1, cyclin-dependent kinase 2 (CDK2), and B-cell CLL/lymphoma 2 (Bcl-2) levels were inhibited with overexpressed-miR-646, while silenced-miR-646 promoted their expression, and the bcl-2-like protein 4 (Bax) level was the opposite. This study found that silenced-IGF1 antagonized the promotive effect of the miR-646 inhibitor on cell proliferation.

Conclusions: MiR-646 inhibitor treatment can promote the proliferation of GCs by regulating the cell cycle and inhibiting apoptosis, while silenced-IGF-1 antagonizes it.

Key words: polycystic ovarian syndrome; granulosa cells; microRNA; miR-646; IGF1; KGN cells

Introduction

Polycystic ovarian syndrome (PCOS) is the most common endocrinopathy in women during their reproductive ages, and depending on different criteria, the prevalence can be up to 6–20% [1–3]. It is clinically characterized by hyperandrogenisms, like acne, seborrhoea, hirsutism, irregular menses, infertility, and alopecia [4]. The diagnosis and treatment of PCOS are not complex, but the pathogenic mechanisms remain obscure, studies have reported that PCOS is associated with insulin resistance and obesity [5, 6]. The ovary is a key organ in PCOS consisting of two steroidogenic cells, tryptophan cells who are responsible for androgen synthesis and granulosa cells (GCs) which are responsible for

the conversion of androgens to estrogens and progesterone synthesis [7]. Sadigh and others reported that the apoptotic and inflammation in the GC were related to the follicle, and the ovarian follicular growth was usually arrested in PCOS [8, 9]. A clinical study reported that oxidative stress can induce the apoptosis of GCs in PCOS patients via the phosphoinositide 3-kinases/protein kinase B (PI3K/Akt) pathway [10]. Additional studies have demonstrated increased proliferation of GCs in the ovaries of anovulatory women compared to normal ovulatory women with PCOS [11]. Similarly, Ji found that the AT-rich interaction domain 1A (ARID1A) is downregulated in GC cells from women and in mouse models with PCOS, and the ARID1A overexpression can inhibit the PI3K/Akt pathway to



Yuefang Ren, Department of Gynaecology, Huzhou Maternity and Child Health Care Hospital, No. 2, East Road, Wuxing District, Huzhou City, Zhejiang Province 313000, China, tel: +86-572-2030026, fax: +86-572-2030060, e-mail: renyuefang9129@sina.com

inhibit the proliferation and promote apoptosis of ovarian GCs [12]. It is seen that regulation of proliferation and apoptosis of GCs is an important mechanism to improve PCOS.

The short non-coding RNAs (miRNAs) play a crucial role in the initiation and progression of PCOS [13]. Bao studied microRNAs (miRNAs) in POCS and found that the expression of miR-130b-3p induced proliferation and inhibit apoptosis in KGN cells, which are positively correlated with the occurrence of PCOS [14]. And the overexpression of some miRNAs can promote apoptosis and inhibit proliferation [15]. The low microRNA 646 (miR-646) expression encouraged the proliferation and migration of ovarian cancer [16], gastric cancer [17], laryngeal carcinoma [18], and endometrial carcinoma [19]. In addition, an increase of insulin-like growth factor (IGF-1) in plasma of PCOS patients has been proven to be related to the insulin resistance, and the expression of IGF-1 was decreased by improving the PCOS [20]. Sirotkin reported that IGF-1 stimulated proliferation and inhibited apoptosis of ovarian cells [21]. Studies have demonstrated the regulation effect of miR-646 on IGF-1 [22]. However, the biological mechanism of miR-646 in PCOS is still unclear.

In this study, we focused on the potential of miR-646 that was down-regulated in POCS patients after the analysis of the Gene Expression Omnibus (GEO) database. We hypothesized that miR-646 has the ability to regulate the proliferation of GCs. Consequently, we investigated the role of the miR-646/IGF1 pathway on GC proliferation by transfecting KGN cells, a kind of human ovarian granulosa cell, with miR-646 mimic and inhibitor.

Material and methods

Bioinformatics analysis

The miRNAs were screened by GEO2R on the GSE86241 of the GEO database. There were 9 control samples and 8 PCOS samples. Using the following filter conditions: $|\text{Log}(\text{FC})| \geq 2$ and $p < 0.05$, 1172 up-regulated and 506 down-regulated miRNAs were obtained. miR-646 is in the top 9 in down-regulated miRNAs according to $|\text{Log}(\text{FC})|$, and was found to be associated with the inhibition of cell proliferation by searching relevant literature. Then the miR-646 was analysed regarding enrichment for biological processes and pathways by FunRich3.1.3 to predict the biological mechanisms.

Cell culture and grouping

Human normal ovarian epithelial cells (IOSE80) and human ovarian granulosa cells (KGN, COV434, SVOG) were purchased from Shanghai iCell Bioscience Inc., China. The F12/DMEM with 10% FBS and 1% penicillin-streptomycin solution were used for culturing cells in 5% CO₂ at 37°C. The KGN cells were transfected by lipofectamine 2000 (11668019, Invitrogen, United States) with miR-646 mimic, miR-646 inhibitor, and si-IGF-1. The corresponding blank vector was used as the control of transfection [23]. The cells were divided into miR-646 mimic-NC, miR-646mimic, miR-646 inhibitor-NC, miR-646 inhibitor, and miR-646 inhibitor + si-IGF-1 groups.

Quantitative real-time PCR (qRT-PCR)

The extraction of miRNA was completed by the miRNA kits (AM1556, Invitrogen, United States). After determining the concentration and purity of miRNA, the reverse transcription was carried out according to the instructions of the miRNA cDNA Synthesis Kit (CW2141, CWBIO, China). Finally, the quantitative real-time polymerase chain reaction (qRT-PCR) and the amplification procedure were carried out according to the instructions of the miRNA qPCR Assay Kit (CW2142, CWBIO, China). In addition, the extraction of total RNA was done through the process of lysis and centrifugation by Trizol (B511311, Sangon, China) and hypothermia high-speed centrifuge (Micro17R, Thermo, United States). The total RNA of cells was dissolved in 40 μL DEPC water, and the concentration and purity were determined by an ultra-micro spectrophotometer (Nanodrop one, Thermo Scientific, United States). HiFiScript cDNA Synthesis Kit (CW2569, CWBIO, China) was used for reverse transcription. After mixing with the SYBR Premix Ex TaqII (RR820A, Takara, Japan) kit, the mixture was put into the qRT-PCR instrument (CFX Connect, BIO-RAD, United States) to start the reaction and the reaction conditions for transcription were set according to the instructions. U6 and GAPDH levels were set as the endogenous control of miR-646 and IGF1. All data were processed by relative quantitative method (2^{- $\Delta\Delta\text{CT}$}). All primer sequences are shown in Table 1.

Cell counting kit-8 (CCK8) assay

The transfected cells were seeded on 96-well plates. After 24, 48, 72, and 96 h of incubation, a 10 μL cell counting kit-8 (CCK-8) (HY-K0301, MCE, United States) was added to each well and incubated for 1 h, and 450 nm was the wavelength at which the microplate reader (CMaxPlus, MD, United States) measured absorbance.

EdU cell proliferation assay

5-ethynyl-2'-deoxyuridine (EdU) cell proliferation assay was used to observe the proliferation of KGN cells [24]. The transfected cells were seeded on 24-well plates. After 48 h of incubation, the adhesive cells were inoculated on the slide that was incubated with 500 μL EdU ($\times 2$) reagents for 2 h according to the instructions of the EdU-594 cell proliferation kit (C0078s, Beyotime, China). After fixing and washing, TritonX-100 was used for incubation for 10 min. Then, the 0.5 mL Click working reagent was added and incubated without light for 30 min. Then, DAPI was used to nuclei stain for 5 min without light. Subsequently, the cells were observed under

Table 1. Primer sequences

Gene	Forward Primer (5'-3')	Reverse Primer (5'-3')
Human miR-646	ATCAGGAGTCTGCCAGTGG	GGCAGCTGCTTCTCTCC
Human IGF-1	GCTCTTCAGTTCGTGTGTGG	GCCTCCTTAGATCACAGCTCC
Human U6	AGTAAGCCCTTGCTGTCACTG	CCTGGGTCTGATAATGCTGGG
Human GAPDH	GGAGCGAGATCCCTCCAAAAT	GGCTGTTGTCATACTTCTCATGG

miR-646 — microRNA 646; IGF-1 — insulin-like growth factor; GAPDH — glyceraldehyde-3-phosphate dehydrogenase

a fluorescent microscope (Ts2-FC, Nikon, Japan). The wavelength of positive cells detecting EdU and DAPI was according to the instructions. Under the fluorescent microscope, the positive cells of EdU were red and the DAPI were blue in appearance.

Cell colony formation assay

The transfected cells were seeded in 12-well plates with 500 cells in each well. The cell culture medium was replaced, and the colony size was observed every third day. When the number of colonies was greater than 50, the cells were washed and fixed with 1 mL 4% paraformaldehyde for 60 mins at 4°C. After 0.1% crystal violet staining for 2 min, the cells were observed and photographed with a microscope (AE2000, Motic, Germany).

Flow cytometry assay

The cell-cycle and apoptosis were measured by flow cytometry (35832442). 6-Well plates were used to culture the cells with 90% confluence. After 48 h of incubation, the cells were washed with ice-PBS buffer and collected in an EP tube. The cells were diluted into 10⁶/mL, and then stained with PI/RNase Staining Buffer (550825, BD Pharmingen, United States) for 30 min away from light. For the cell apoptosis assay, the cells were processed with a FITC Annexin V Apoptosis Detection Kit I (556547, BD Pharmingen, United States) for 15 min away from light. The distribution of the cell cycle and apoptosis were detected using a flow cytometer (C6, BD Pharmingen, United States).

Western blot

After extraction and denaturation of total protein from cells, the 10% gel electrophoresis and activated polyvinylidene difluoride (PVDF) membranes were used for Western blot. Then the blocked membranes were incubated with primary antibodies, including anti-cyclin D1 (1:2000, AF0931, Affinity, United States), anti-cyclin-dependent kinase 2 (CDK2) (1:2000, AF6237, Affinity, United States), anti-bcl-2-like protein 4 (Bax) (1:3000, AF0120, Affinity, United States), anti-B-cell CLL/lymphoma 2 (Bcl-2) (1:2000, AF6139, Affinity, United States), anti-IGF-1 (1:2000, AF6124, Affinity, United States), anti-actin (1:20,000, AF7018, Affinity, United States), and anti-GAPDH (1:20,000, AF7021, Affinity, United States) followed by a corresponding secondary antibody (1:10,000, S0001/2, Affinity, United States) at room temperature for 1.5 h. The membrane was incubated with enhanced chemiluminescence (ECL) reagents (610020-9Q, Qing Xiang, China) and visualized by ImageJ software.

Statistical analysis

The data were analysed by SPSS 19.0 and the results of the continuous variables are presented as the mean \pm standard deviation (SD). The Turkey test was used to analyse the measurement data that conforms to the normal distribution and homogeneous variance. The independent sample *t*-test was used to analyse the measurement data that conforms to the normal distribution with the variance being uneven. And the Kruskal-Wallis H test was used to analyse the measurement data that does not conform to the normal distribution. $p < 0.05$ was considered to be statistically significant.

Results

Screening of miRNAs associated with the PCOS based on the GEO database by bioinformatic techniques

There were 1172 up-regulated (green) and 506 down-regulated (red) miRNAs in the PCOS patients compared to the control group (Fig. 1A). In 506

down-regulated miRNAs, the top 10 miRNAs in FC value are shown in Figure 1B. The miR-646 is predicted to participate in the transport, the cell communication, the signal transduction, and the regulation of nucleobase nucleoside, nucleotide, and nucleic acid metabolism ($p < 0.05$) (Fig. 1C). MiR-646 was related to the insulin, class I PI3K signalling events mediated by AKT, mammalian target of rapamycin (mTOR) signalling, and IGF-1 pathways (Fig. 1D). Then, the qRT-PCR was used to screen the cells for further exploration. In the KGN cells, the miR-646 level was the lowest ($p < 0.05$) and the IGF-1 mRNA level was the highest ($p < 0.01$), compared to the IOSE80 cells (Fig. 2A and 2B).

The effect of regulating miRNA-646 on the proliferation of KGN cells

As shown in Figure 2C, after overexpressed miR-646, the miR-646 level was up-regulated in KGN cells ($p < 0.01$). Conversely, the miR-646 level was down-regulated in KGN cells after silenced miR-646 ($p < 0.01$). In addition, the CCK-8 was used for measuring the cell viability to reflect the level of cell proliferation indirectly. At 48, 72, and 96 h the miR-646 mimic treatment on the KGN cells inhibited cell viability immensely ($p < 0.05$ and $p < 0.01$) (Fig. 2D). While, after the same processing time, the cell viability was raised markedly with miR-646 inhibitor treatment ($p < 0.01$) (Fig. 2D). Also, the EdU method is always used to observe the proliferation, and the results of the relative EdU-positive cells were reduced in the miR-646 mimic group compared to the miR-646 mimic-NC group ($p < 0.01$) (Fig. 2E). The relative EdU-positive cells were raised markedly with miR-646 inhibitor treatment ($p < 0.01$) (Fig. 2F).

The effect of regulating miRNA-646 on colony number, cell cycle, and apoptosis of KGN cells

The colony number was observed by cell clone formation assay (Fig. 3A). The colony number of KGN cells decreased markedly with the miR-646 mimic treatment, while the colony number of KGN cells with miR-646 inhibitor treatment was increased ($p < 0.01$). The cell cycle and apoptosis were explored by flow cytometry assay. With miR-646 mimic treatment, the cell number in the S stage was inhibited, and in the G2/M stage it was raised significantly ($p < 0.01$ and $p < 0.05$). However, the cell number in the S stage with the miR-646 inhibitor treatment was raised, and in the G2/M was inhibited ($p < 0.01$). What is more, the apoptosis of KGN cells with miR-646 mimic treatment was raised enormously, and the miR-646 inhibitor treatment reduced it markedly ($p < 0.01$) (Fig. 3BC).

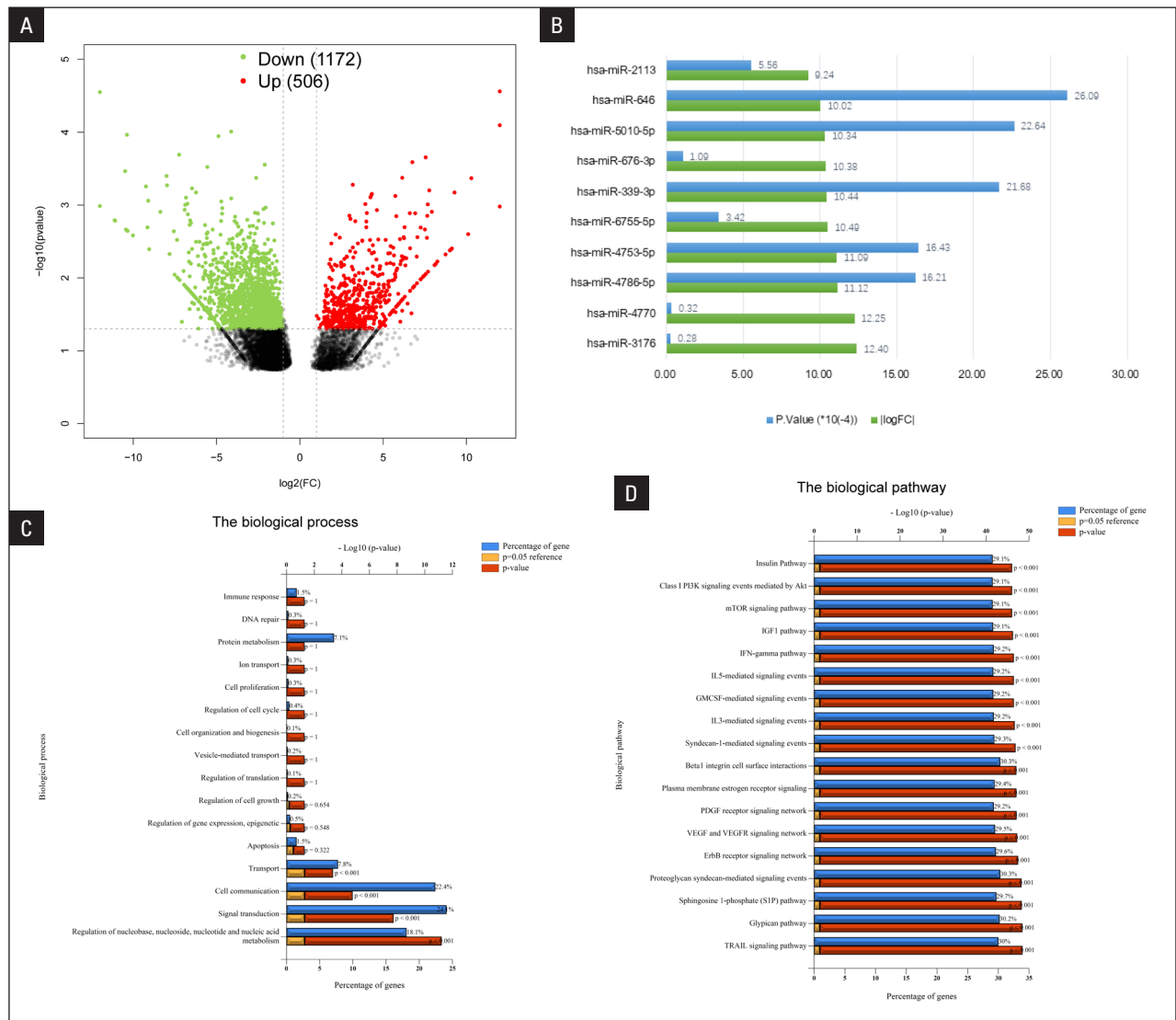


Figure 1. The results of bioinformatics analysis based on the Gene Expression Omnibus (GEO) database. **A.** The volcano map of the up-/down-regulated miRNAs that compared polycystic ovarian syndrome (PCOS) to the control with significant differences in GSE86241 DataSets from GEO. Filter conditions are $|\log(\text{FC})| \geq 2$ and $p < 0.05$. There are 1172 up-regulated (green) and 506 down-regulated (red) miRNAs; **B.** The top 10 miRNA of the down-regulated in the PCOS patients compared to the control. The length of the green bar means the absolute value of the $|\log(\text{FC})|$, and the length of the blue bar means the p-value; **C.** The biological process of the miR-646; **D.** The biological pathway for miR-646; FC — fold change

MiRNA-646 targets IGF-1 and regulates the cell cycle/apoptosis-related protein levels

The effect of miRNA-646 targeting on IGF1 was identified by a dual-luciferase reporter assay. After binding IGF1 to the 3'-UTR of miR-646, the relative luciferase activity was inhibited markedly in the WT group compared to the NC group, but it had no significant difference after the IGF-1 mutation ($p < 0.01$) (Fig. 4A). Also, the transcription and translation levels of IGF-1 were inhibited by the miR-646 mimic treatment and were raised by the miR-646 inhibitor treatment ($p < 0.01$) (Fig. 4B–D). Interestingly, by the miR-646 mimic treatment, the expression degree of Cyclin D1, CDK2,

and Bcl-2 proteins were reduced markedly ($p < 0.01$ and $p < 0.05$), and the Bax protein level was increased notably ($p < 0.01$) (Fig. 4E–H). The effect of miR-646 inhibitor treatment on those proteins was completely opposite ($p < 0.05$ or $p < 0.01$).

IGF1 silencing antagonises the effects of miR-646 inhibitor treatment on the colony number and cell viability of KGN cells

In KGN cells with miR-646 inhibitor treatment, the colony number was increased ($p < 0.01$) (Fig. 5AB), and the cell viability at 48, 72, and 96 h was raised also ($p < 0.05$ and $p < 0.01$) (Fig. 5C), while IGF1 silencing

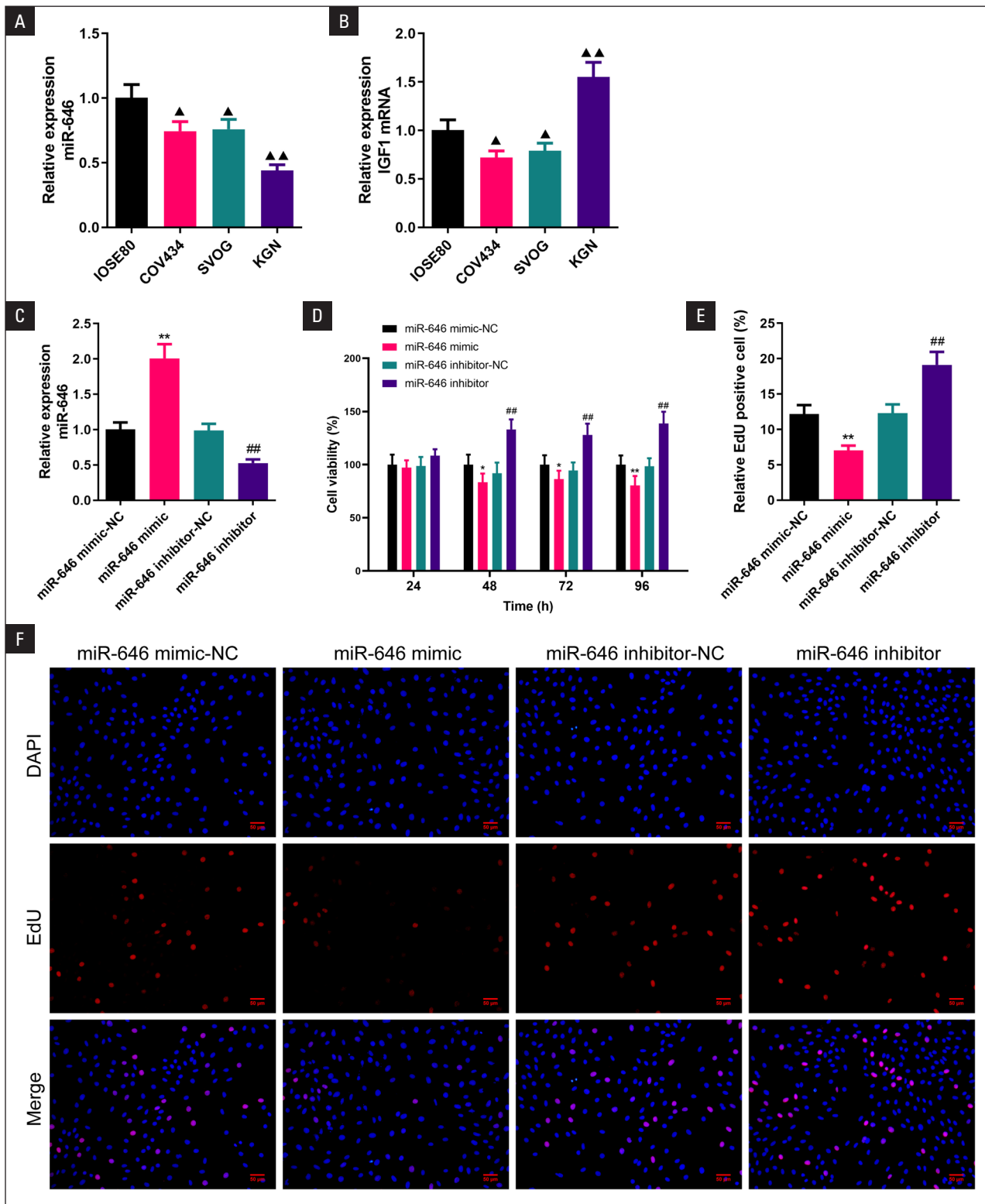


Figure 2. The effect of microRNA 646 (miRNA-646) on the proliferation of human ovarian granular cells. **AB.** The levels of miR-646 and insulin-like growth factor (IGF-1) mRNA in the IOSE80, COV434, SVOG, and KGN cells were measured by quantitative real-time polymerase chain reaction (qRT-PCR) ($n = 3$); **C.** The levels of miR-646 in the KGN cells after transfection with mimic and inhibitor of miR-646 were measured by qRT-PCR ($n = 3$); **D.** The cell viability of transfected-miRNA-646 mimic/inhibitor in KGN cells at 24, 48, 72, and 96 hours was measured by cell counting kit-8 (CCK-8) ($n = 5$); **EE.** The proliferation levels and representative photos of cells with transfected-miRNA-646 mimic/inhibitor were detected by the 5-ethynyl-2'-deoxyuridine (EdU) method (200 \times , $n = 3$). Data are presented as the mean \pm standard deviation. [▲] $p < 0.05$, ^{▲▲} $p < 0.01$ vs. IOSE80 group; ^{*} $p < 0.05$, ^{**} $p < 0.01$ vs. miR-646 mimic-NC group; [#] $p < 0.05$, ^{##} $p < 0.01$ vs. miR-646 inhibitor-NC group

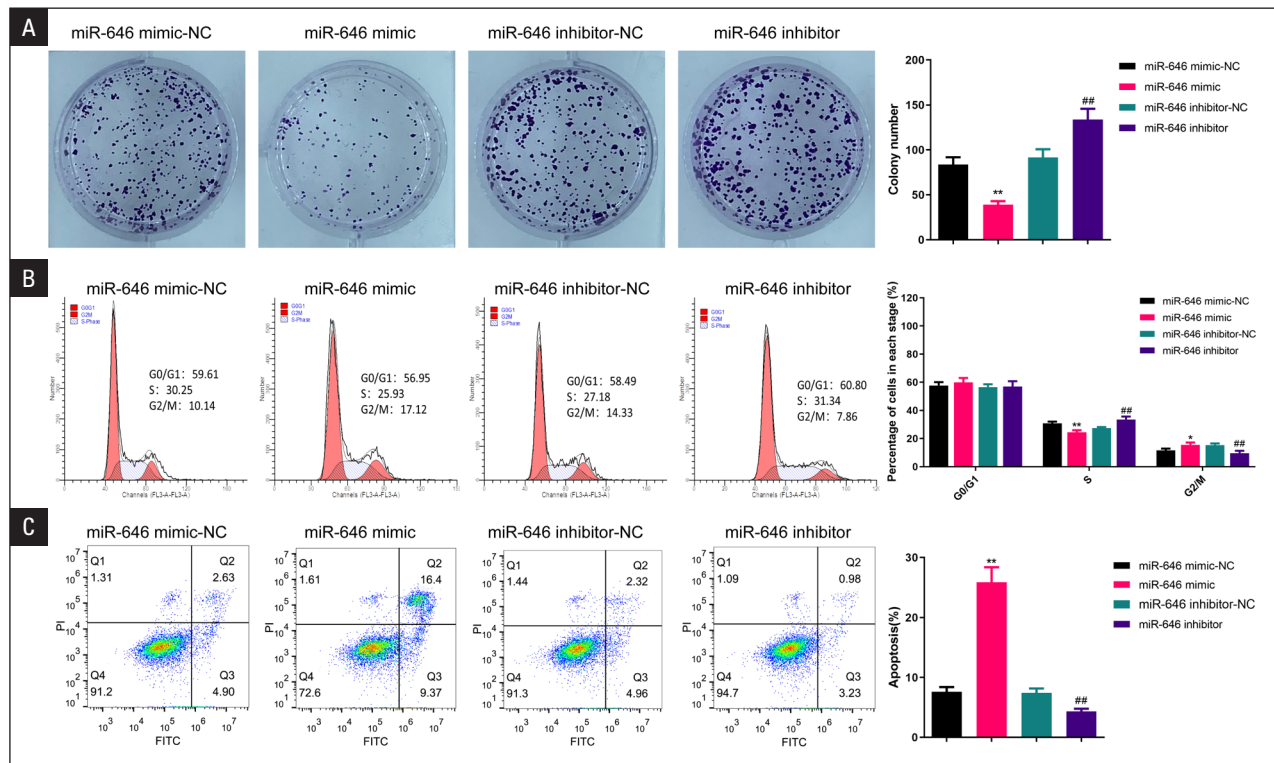


Figure 3. The effect of microRNA 646 (miRNA-646) on colony number, cell cycle, and apoptosis of KGN cells; **A.** The colony number of KGN cells with transfected-miRNA-646 mimic/inhibitor was observed by cell clone formation assay ($n = 3$); The cell cycle (**B**) and apoptosis (**C**) of KGN cells with transfected-miRNA-646 mimic/inhibitor were measured by flow cytometry analysis ($n = 3$). Data are presented as the mean \pm standard deviation. * $p < 0.05$, ** $p < 0.01$ vs. miR-646 mimic-NC group; # $p < 0.05$, ## $p < 0.01$ vs. miR-646 inhibitor-NC group

antagonized the effects of miR-646 inhibitor treatment on KGN cells ($p < 0.01$ and $p < 0.05$) (Fig. 5BC).

Discussion

PCOS is the most prevalent reason for anovulatory infertility and hyperandrogenism. Research suggests that insulin resistance and compensatory hyperinsulinaemia are perhaps the predominant and primary defects in PCOS [24]. The balance of proliferation and apoptosis of GCs is crucial for PCOS women. Li studied the GCs from 96 PCOS women and 58 healthy women and found high expression of the high-mobility group AT-hook 2 (HMGA2) and IGF2 mRNA in PCOS women and proved that the HMGA2/ IGF2 mRNA binding protein 2 (IMP2) pathway promoted the proliferation of GCs *in vitro* [11]. While Zheng's team studied the down-regulated atrial natriuretic peptide (ANP) in PCOS patients and found ANP can promote the proliferation of GCs *in vitro* and *in vivo*, and ANP treatment reversed most of the symptoms in PCOS rats [25]. It can be seen that the role of proliferation in GCs in the occurrence and development of PCOS is very complex, so it is necessary to explore the biological

mechanism of proliferation in GCs for the treatment of PCOS.

In this study, we obtained miRNAs that are related to the PCOS patients through the GSE86241 of the GEO database. Of these, the down-regulated miR-646 was proven to be associated with proliferation in breast cancer and human periodontal ligament cells [22]. Also, in this paper, the down-regulated miR-646 was proven to be involved in the insulin pathway by pathway enrichment analysis. Similarly, we proved the inhibition effect of up-regulated miR-646 in the proliferation of GCs and vice versa. Most tissue development needs to strike a balance between apoptosis and cell proliferation. Therefore, the effect of miR-646 on apoptosis in GCs was also studied by flow cytometry, and it was found that its trend was inversely proportional to proliferation. What is more, the level of Bax – the pro-apoptosis proteins [26], was directly proportional to the expression of miR-646, and Bcl-2 had the opposite trend. It was further proven that miR-646 inhibited the proliferation of KGN cells by promoting apoptosis.

The proliferation of somatic cells was performed through the mitotic process, which is determined by the progress of the cell cycle [27]. Interestingly, we

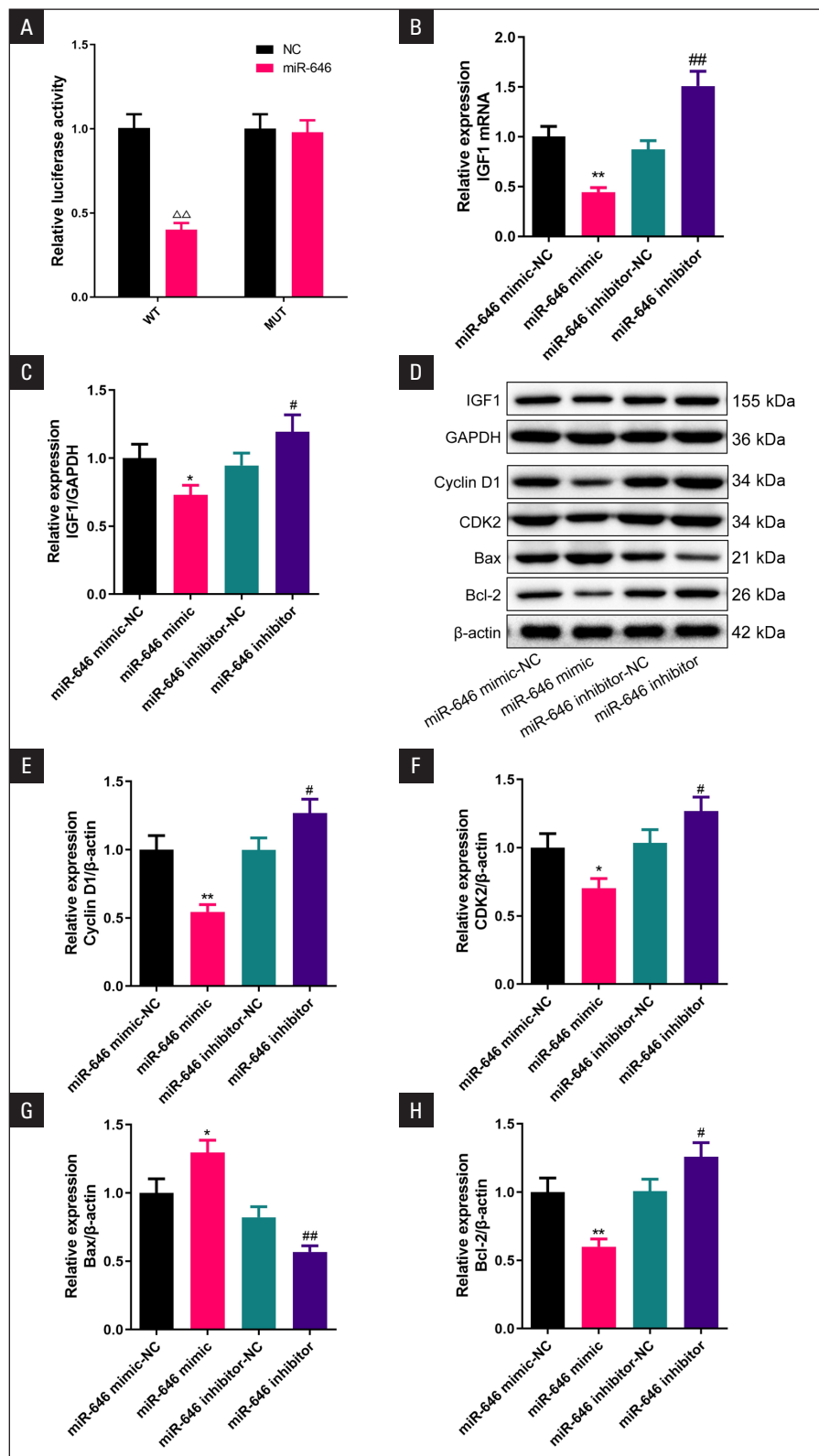


Figure 4. The effect of microRNA 646 (miRNA-646) on the transcription and translation level of insulin growth factor (IGF-1), and the cell cycle/apoptosis-related protein levels in the KGN cells. **A.** The effect of miRNA-646 on IGF-1 transcription was investigated by a dual-luciferase reporter assay ($n = 3$); **BC.** The levels of IGF-1 mRNA and protein in the KGN cells after transfection with mimic and inhibitor of miR-646 were measured by quantitative real-time polymerase chain reaction (qRT-PCR) and Western blot ($n = 3$); **D.** The protein band profiles of Western blot. And the levels of cyclin D1 (**E**), cyclin-dependent kinase 2 (CDK2) (**F**), bcl-2-like protein 4 (Bax) (**G**), and B-cell CLL/lymphoma 2 (Bcl-2) (**H**) proteins were analysed by Western blot ($n = 3$). Data are presented as the mean \pm standard deviation. $\Delta\Delta p < 0.01$ vs. NC group; $*p < 0.05$, $**p < 0.01$ vs. miR-646 mimic-NC group; $\#p < 0.05$, $##p < 0.01$ vs. miR-646 inhibitor-NC group

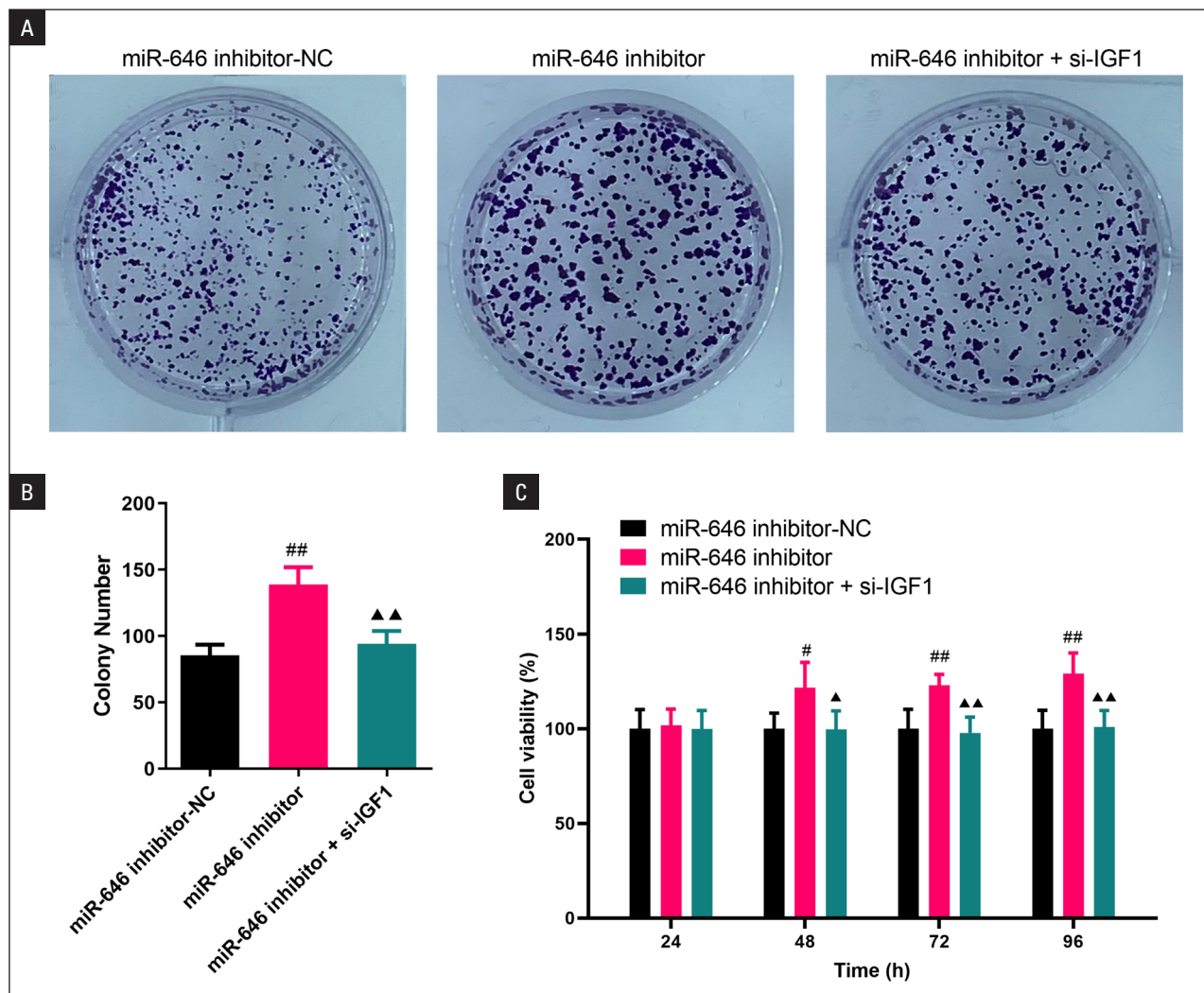


Figure 5. The effect of of microRNA 646 (miR-646) inhibitor on the colony number and cell viability of KGN cells via insulin-like growth factor (IGF-1). **AB.** The effect of si-IGF1 on colony number in the KGN cells with miRNA-646 knockdown was observed by cell clone formation assay ($n = 3$). **C.** At 24, 48, 72, and 96 hours, the effect of si-IGF1 on the cell viability in the KGN cells with miRNA-646 knockdown was measured by cell counting kit-8 (CCK-8) ($n = 3$). Data are presented as the mean \pm standard deviation (SD). $\#p < 0.05$, $\#\#p < 0.01$ vs. miR-646 inhibitor-NC group; $\blacktriangle p < 0.05$, $\blacktriangle\blacktriangle p < 0.01$ vs. miR-646 inhibitor group

found that overexpression or inhibition of miR-646 affected the number of cells in the S and G2/M phases of cell cycle. We also found the proteins cyclin D1 and CDK2, which were related to cell cycle, were inhibited with miR-646 mimic treatment, while miR-646 inhibitor treatment on KGN cells increased them. Cyclin D1 plays a crucial role in G1-S cell cycle transition, and the decrease of its level will lead to the decrease of proliferation [28]. Cyclin D1 was proven to be a direct regulator of both proliferative and immature states of cerebellar granule cell progenitors [29]. Also, Spencer et al. constructed a living cell sensor for CDK2 activity and found that many cells immediately commit to the next cell cycle by building up CDK2 activity from an intermediate level, while other cells lack CDK2 activity and enter a transient state of quiescence [30]. It is suggested that miR-646 may regulate prolifera-

tion and apoptosis by affecting cell cycle-associated proteins.

Generally speaking, the proliferation and differentiation of GCs lead to follicular maturation and ovulation, while the apoptosis and degeneration of GC lead to follicular atresia [31]. IGF-1 has been proven to antagonize the apoptosis of GCs, and the Bcl-2/Bax of GCs were advanced by IGF-1 treatment [32]. A study found that dehydroepiandrosterone can increase the level of IGF-1 in serum to induce PCOS in C57BL/6 mice [33]. This study found that the silenced IGF-1 inhibited the colony number and viability in the GCs that were transfected with miR-646 inhibitor. It indicates that miR-646 regulates proliferation of GCs by promoting the expression of IGF-1. In conclusion, this study found that down-regulated miR-646 regulates proliferation of GC cells through activation of IGF-1.

Conclusion

In this study, the inhibitory effect of miR-646 on the proliferation, cloning ability and apoptosis, and the regulation effect on the S and G2/M stages of the cell cycle in human ovarian granular cells was proven. Also, by miR-646-overexpression, the levels of IGF-1, cyclin D1, CDK2, and Bcl-2 were inhibited, and the Bax level was raised. This demonstrates that the inhibitory effect of miR-646 on proliferation may be related to regulation of the cell cycle and apoptosis. In addition, silenced-IGF-1 antagonized the promoting effect of the miR-646 inhibitor on the colony number and proliferation of KGN cells, which proved that miR-646 inhibited the proliferation of ovarian granulosa cells via IGF-1. In conclusion, this study provides a foundation for the study of miRNAs in PCOS and a new direction for the treatment of PCOS.

Conflict of interest

All authors declare there are no financial interests in the information contained in the manuscript.

Authors' contributions

Conception and design of the research by J.L.L. Acquisition of data and statistical analysis by F.L.X. and A.X.C. Manuscript drafting by R.Y.J. and W.M.Z. Manuscript revision by Y.J.Y. and Y.F.R. Funding obtained by J.L.L.

Acknowledgements

This study was supported by Huzhou Science and Technology Plan Project (2022GYB56).

References

- Goodarzi MO, Dumesic DA, Chazenbalk G, et al. Polycystic ovary syndrome: etiology, pathogenesis and diagnosis. *Nat Rev Endocrinol.* 2011; 7(4): 219–231, doi: [10.1038/nrendo.2010.217](https://doi.org/10.1038/nrendo.2010.217), indexed in Pubmed: [21263450](https://pubmed.ncbi.nlm.nih.gov/21263450/).
- Anagnostis P, Tarlatzis BC, Kauffman RP. Polycystic ovarian syndrome (PCOS): Long-term metabolic consequences. *Metabolism.* 2018; 86: 33–43, doi: [10.1016/j.metabol.2017.09.016](https://doi.org/10.1016/j.metabol.2017.09.016), indexed in Pubmed: [29024702](https://pubmed.ncbi.nlm.nih.gov/29024702/).
- Wolf WM, Wattick RA, Kinkade ON, et al. Geographical Prevalence of Polycystic Ovary Syndrome as Determined by Region and Race/Ethnicity. *Int J Environ Res Public Health.* 2018; 15(11), doi: [10.3390/ijerph15112589](https://doi.org/10.3390/ijerph15112589), indexed in Pubmed: [30463276](https://pubmed.ncbi.nlm.nih.gov/30463276/).
- Madnani N, Khan K, Chauhan P, et al. Polycystic ovarian syndrome. *Indian J Dermatol Venereol Leprol.* 2013; 79(3): 310–321, doi: [10.4103/0378-6323.110759](https://doi.org/10.4103/0378-6323.110759), indexed in Pubmed: [23619436](https://pubmed.ncbi.nlm.nih.gov/23619436/).
- Escobar-Morreale HF. Polycystic ovary syndrome: definition, aetiology, diagnosis and treatment. *Nat Rev Endocrinol.* 2018; 14(5): 270–284, doi: [10.1038/nrendo.2018.24](https://doi.org/10.1038/nrendo.2018.24), indexed in Pubmed: [29569621](https://pubmed.ncbi.nlm.nih.gov/29569621/).
- Zeng X, Xie YJ, Liu YT, et al. Polycystic ovarian syndrome: Correlation between hyperandrogenism, insulin resistance and obesity. *Clin Chim Acta.* 2020; 502: 214–221, doi: [10.1016/j.cca.2019.11.003](https://doi.org/10.1016/j.cca.2019.11.003), indexed in Pubmed: [31733195](https://pubmed.ncbi.nlm.nih.gov/31733195/).
- Havelock JC, Rainey WE, Carr BR. Ovarian granulosa cell lines. *Mol Cell Endocrinol.* 2004; 228(1–2): 67–78, doi: [10.1016/j.mce.2004.04.018](https://doi.org/10.1016/j.mce.2004.04.018), indexed in Pubmed: [15541573](https://pubmed.ncbi.nlm.nih.gov/15541573/).
- Raei Sadigh A, Darabi M, Salmassi A, et al. Fractalkine and apoptotic/anti-apoptotic markers in granulosa cells of women with polycystic ovarian syndrome. *Mol Biol Rep.* 2020; 47(5): 3593–3603, doi: [10.1007/s11033-020-05452-0](https://doi.org/10.1007/s11033-020-05452-0), indexed in Pubmed: [32350744](https://pubmed.ncbi.nlm.nih.gov/32350744/).
- Chahal N, Geethadevi A, Kaur S, et al. Direct impact of gonadotropins on glucose uptake and storage in preovulatory granulosa cells: Implications in the pathogenesis of polycystic ovary syndrome. *Metabolism.* 2021; 115: 154458, doi: [10.1016/j.metabol.2020.154458](https://doi.org/10.1016/j.metabol.2020.154458), indexed in Pubmed: [33278413](https://pubmed.ncbi.nlm.nih.gov/33278413/).
- Gong Y, Luo S, Fan P, et al. Growth hormone activates PI3K/Akt signaling and inhibits ROS accumulation and apoptosis in granulosa cells of patients with polycystic ovary syndrome. *Reprod Biol Endocrinol.* 2020; 18(1): 121, doi: [10.1186/s12958-020-00677-x](https://doi.org/10.1186/s12958-020-00677-x), indexed in Pubmed: [33287836](https://pubmed.ncbi.nlm.nih.gov/33287836/).
- Li M, Zhao H, Zhao SG, et al. The HMGA2-IMP2 Pathway Promotes Granulosa Cell Proliferation in Polycystic Ovary Syndrome. *J Clin Endocrinol Metab.* 2019; 104(4): 1049–1059, doi: [10.1210/je.2018-00544](https://doi.org/10.1210/je.2018-00544), indexed in Pubmed: [30247605](https://pubmed.ncbi.nlm.nih.gov/30247605/).
- Ji XL, Liu X, Wang Z, et al. Expression of ARID1A in polycystic ovary syndrome and its effect on the proliferation and apoptosis of ovarian granulosa cells. *Ann Endocrinol (Paris).* 2020; 81(6): 521–529, doi: [10.1016/j.ando.2020.11.008](https://doi.org/10.1016/j.ando.2020.11.008), indexed in Pubmed: [33290750](https://pubmed.ncbi.nlm.nih.gov/33290750/).
- Chen B, Xu P, Wang J, et al. The role of MiRNA in polycystic ovary syndrome (PCOS). *Gene.* 2019; 706: 91–96, doi: [10.1016/j.gene.2019.04.082](https://doi.org/10.1016/j.gene.2019.04.082), indexed in Pubmed: [31054362](https://pubmed.ncbi.nlm.nih.gov/31054362/).
- Bao D, Li M, Zhou D, et al. miR-130b-3p is high-expressed in polycystic ovarian syndrome and promotes granulosa cell proliferation by targeting SMAD4. *J Steroid Biochem Mol Biol.* 2021; 209: 105844, doi: [10.1016/j.jsmb.2021.105844](https://doi.org/10.1016/j.jsmb.2021.105844), indexed in Pubmed: [33582305](https://pubmed.ncbi.nlm.nih.gov/33582305/).
- Jiang YC, Ma JX. The role of MiR-324-3p in polycystic ovary syndrome (PCOS) via targeting WNT2B. *Eur Rev Med Pharmacol Sci.* 2018; 22(11): 3286–3293, doi: [10.26355/eurev.201806_15147](https://doi.org/10.26355/eurev.201806_15147), indexed in Pubmed: [29917177](https://pubmed.ncbi.nlm.nih.gov/29917177/).
- Sun D, Liu J, Zhou L. Upregulation of circular RNA circFAM53B predicts adverse prognosis and accelerates the progression of ovarian cancer via the miR646/VAMP2 and miR647/MDM2 signaling pathways. *Oncol Rep.* 2019; 42(6): 2728–2737, doi: [10.3892/or.2019.7366](https://doi.org/10.3892/or.2019.7366), indexed in Pubmed: [31638250](https://pubmed.ncbi.nlm.nih.gov/31638250/).
- Zhang P, Tang WM, Zhang H, et al. MiR-646 inhibited cell proliferation and EMT-induced metastasis by targeting FOXK1 in gastric cancer. *Br J Cancer.* 2017; 117(4): 525–534, doi: [10.1038/bjc.2017.181](https://doi.org/10.1038/bjc.2017.181), indexed in Pubmed: [28632723](https://pubmed.ncbi.nlm.nih.gov/28632723/).
- Yuan X, Liu Y, Chen E, et al. MiR-646 regulates proliferation and migration of laryngeal carcinoma through the PI3K/AKT pathway via targeting GPX1. *Oral Dis.* 2021; 27(7): 1678–1686, doi: [10.1111/odi.13706](https://doi.org/10.1111/odi.13706), indexed in Pubmed: [33150676](https://pubmed.ncbi.nlm.nih.gov/33150676/).
- Wang Bo, Lu Ye, Feng E. hsa_circ_0001610 knockdown modulates miR-646-STAT3 axis to suppress endometrial carcinoma progression. *J Gene Med.* 2021; 23(6): e3337, doi: [10.1002/jgm.3337](https://doi.org/10.1002/jgm.3337), indexed in Pubmed: [33822442](https://pubmed.ncbi.nlm.nih.gov/33822442/).
- Farhadi-Azar M, Ghahremani M, Mahboobifard F, et al. Effects of Rosa damascena on reproductive improvement, metabolic parameters, liver function and insulin-like growth factor-1 gene expression in estradiol valerate induced polycystic ovarian syndrome in Wistar rats. *Biomed J.* 2022 [Epub ahead of print], doi: [10.1016/j.bj.2022.05.003](https://doi.org/10.1016/j.bj.2022.05.003), indexed in Pubmed: [35605922](https://pubmed.ncbi.nlm.nih.gov/35605922/).
- Sirotkin A, Alexa R, Kádasi A, et al. Resveratrol directly affects ovarian cell sirtuin, proliferation, apoptosis, hormone release and response to follicle-stimulating hormone (FSH) and insulin-like growth factor I (IGF-I). *Reprod Fertl Dev.* 2019 [Epub ahead of print], doi: [10.1071/RD18425](https://doi.org/10.1071/RD18425), indexed in Pubmed: [30975285](https://pubmed.ncbi.nlm.nih.gov/30975285/).
- Yang J, Zhou J, Cui B, et al. Evaluation of Hypoxia on the Expression of miR-646/IGF-1 Signaling in Human Periodontal Ligament Cells (hP-DLCs). *Med Sci Monit.* 2018; 24: 5282–5291, doi: [10.12659/MSM.910163](https://doi.org/10.12659/MSM.910163), indexed in Pubmed: [30058629](https://pubmed.ncbi.nlm.nih.gov/30058629/).
- Wang Z. The guideline of the design and validation of MiRNA mimics. *Methods Mol Biol.* 2011; 676: 211–223, doi: [10.1007/978-1-60761-863-8_15](https://doi.org/10.1007/978-1-60761-863-8_15), indexed in Pubmed: [20931400](https://pubmed.ncbi.nlm.nih.gov/20931400/).
- Zhang Z, Li J, Huang Y, et al. Upregulated miR-1258 regulates cell cycle and inhibits cell proliferation by directly targeting E2F8 in CRC. *Cell Prolif.* 2018; 51(6): e12505, doi: [10.1111/cpr.12505](https://doi.org/10.1111/cpr.12505), indexed in Pubmed: [30144184](https://pubmed.ncbi.nlm.nih.gov/30144184/).
- Zheng Q, Li Y, Zhang D, et al. ANP promotes proliferation and inhibits apoptosis of ovarian granulosa cells by NPRA/PGRMC1/EGFR complex and improves ovary functions of PCOS rats. *Cell Death Dis.* 2017; 8(10): e3145, doi: [10.1038/cddis.2017.494](https://doi.org/10.1038/cddis.2017.494), indexed in Pubmed: [29072679](https://pubmed.ncbi.nlm.nih.gov/29072679/).
- Guo M, Lv M, Shao Y, et al. Bax functions as coelomocyte apoptosis regulator in the sea cucumber *Apostichopus japonicus*. *Dev Comp Immunol.* 2020; 102: 103490, doi: [10.1016/j.dci.2019.103490](https://doi.org/10.1016/j.dci.2019.103490), indexed in Pubmed: [31494220](https://pubmed.ncbi.nlm.nih.gov/31494220/).
- Alenzi FQB. Links between apoptosis, proliferation and the cell cycle. *Br J Biomed Sci.* 2004; 61(2): 99–102, doi: [10.1080/09674845.2004.11732652](https://doi.org/10.1080/09674845.2004.11732652), indexed in Pubmed: [15250676](https://pubmed.ncbi.nlm.nih.gov/15250676/).
- O'Connor MJ, Thakar T, Nicolae CM, et al. PARP14 regulates cyclin D1 expression to promote cell-cycle progression. *Oncogene.* 2021; 40(30): 4872–4883, doi: [10.1038/s41388-021-01881-8](https://doi.org/10.1038/s41388-021-01881-8), indexed in Pubmed: [34158578](https://pubmed.ncbi.nlm.nih.gov/34158578/).
- Miyashita S, Owa T, Seto Y, et al. Cyclin D1 controls development of cerebellar granule cell progenitors through phosphorylation and stabilization of ATOH1. *EMBO J.* 2021; 40(14): e105712, doi: [10.15252/embj.2020105712](https://doi.org/10.15252/embj.2020105712), indexed in Pubmed: [34057742](https://pubmed.ncbi.nlm.nih.gov/34057742/).

30. Spencer SL, Cappell SD, Tsai FC, et al. The proliferation-quiescence decision is controlled by a bifurcation in CDK2 activity at mitotic exit. *Cell*. 2013; 155(2): 369–383, doi: [10.1016/j.cell.2013.08.062](https://doi.org/10.1016/j.cell.2013.08.062), indexed in Pubmed: [24075009](https://pubmed.ncbi.nlm.nih.gov/24075009/).
31. Zhang J, Xu Y, Liu H, et al. MicroRNAs in ovarian follicular atresia and granulosa cell apoptosis. *Reprod Biol Endocrinol*. 2019; 17(1): 9, doi: [10.1186/s12958-018-0450-y](https://doi.org/10.1186/s12958-018-0450-y), indexed in Pubmed: [30630485](https://pubmed.ncbi.nlm.nih.gov/30630485/).
32. Han Y, Wang S, Wang Y, et al. IGF-1 Inhibits Apoptosis of Porcine Primary Granulosa Cell by Targeting Degradation of Bim. *Int J Mol Sci*. 2019; 20(21), doi: [10.3390/ijms20215356](https://doi.org/10.3390/ijms20215356), indexed in Pubmed: [31661816](https://pubmed.ncbi.nlm.nih.gov/31661816/).
33. Dou L, Zheng Y, Li Lu, et al. The effect of cinnamon on polycystic ovary syndrome in a mouse model. *Reprod Biol Endocrinol*. 2018; 16(1): 99, doi: [10.1186/s12958-018-0418-y](https://doi.org/10.1186/s12958-018-0418-y), indexed in Pubmed: [30340496](https://pubmed.ncbi.nlm.nih.gov/30340496/).